

Prediction of rail ballast breakage using a hybrid ML methodology

Srinivas Alagesan^a, Buddhima Indraratna^{b,*}, Rakesh Sai Malisetty^a, Yujie Qi^c,
Cholachat Rujikiatkamjorn^d

^a School of Civil and Environmental Engineering, University of Technology Sydney, Ultimo, Australia

^b Distinguished Professor of Civil Engineering and Director of Transport Research Centre, University of Technology Sydney, Ultimo, Australia

^c Transport Research Centre (TRC), University of Technology Sydney (UTS), 15 Broadway, Ultimo NSW 2007, Australia

^d Transport Research Centre, School of Civil and Environmental Engineering, University of Technology Sydney, Ultimo, NSW 2007, Australia

ARTICLE INFO

Keywords:

Artificial neural networks
Ballast breakage
Cyclic loading
Genetic algorithm
Railway track

ABSTRACT

Particle breakage is a key performance indicator to estimate ballast degradation as it severely affects the performance and maintenance of rail tracks. Most constitutive models usually based on continuum mechanics have rarely been able to estimate the rate and intensity of particle degradation under repeated wheel loading. In this regard, this paper presents a novel model for predicting ballast breakage under prolonged cyclic loading using artificial neural networks (ANN) coupled with a genetic algorithm (GA), hence the acronym GA-ANN. For this study, a comprehensive database consisting of 130 experimental datasets on ballast breakage under cyclic loading conditions is used. Unlike most black-box type machine learning (ML) models, this study incorporates a knowledge-guided selection of 9 input parameters encompassing gradation characteristics, particle angularity, the initial physical state of the granular assembly, and the applied stress state. To overcome limitations associated with potential overfitting when using smaller datasets of the Ballast Breakage Index (BBI), this study employs an innovative approach by integrating k-fold cross-validation and regularization with conventional GA-ANN algorithm. The proposed GA-ANN model showed superior performance in predicting BBI at different loading cycles and proved to be 50% more efficient when compared to conventional ANN and other ML techniques. When verified against unseen laboratory and field data, the GA-ANN model yielded an R^2 between 0.85 and 0.95, thus proving its broader capability. Further, global sensitivity analysis is performed to identify the most significant parameters (cyclic deviatoric stress, number of load cycles and frequency) which warrant more attention during maintenance.

Introduction

The rapid expansion of Australian railway infrastructure in the 21st century necessitates prudent planning of maintenance activities to efficiently cater for both passenger and freight transportation. Ballast is the uppermost granular layer in a railway track and acts as the primary load-bearing stratum to resist and distribute the loads from moving trains, while also providing free drainage for the track. Under repetitive loading, the angular corners of ballast aggregates break into finer particles, eventually reducing the internal friction angle while impeding its drainage capacity. In Australia, a significant portion of track maintenance has been attributed to the replacement of the degraded ballast layer due to broken ballast aggregates [24,61]. Previous researchers

have extensively explored the evolution of ballast breakage with time under varied subgrade and loading conditions through large-scale laboratory and field studies [22,31,1,53,26]. Embracing the recent emergence of machine learning (ML) in railway geotechnical applications and using them to efficiently analyse complex datasets can highlight and predict hidden relationships between ballast breakage and its influencing factors. Development of such models helps optimise the amount of laborious experimental testing and facilitates data-driven decision-making to minimise track maintenance costs.

Particle breakage of ballast can be quantified using Ballast Breakage Index (BBI) which is calculated based on the change in particle size distribution before and after cyclic loading [23]. BBI was typically determined through large-scale laboratory tests to study its evolution

* Corresponding author at: School of Civil and Environmental Engineering, Faculty of Engineering and Information Technology, University of Technology Sydney, Australia.

E-mail addresses: srinivas.alagesan@student.uts.edu.au (S. Alagesan), buddhima.indraratna@uts.edu.au (B. Indraratna), rakeshsai.malisetty@uts.edu.au (R.S. Malisetty), yujie.qi@uts.edu.au (Y. Qi), cholachat.rujikiatkamjorn@uts.edu.au (C. Rujikiatkamjorn).

<https://doi.org/10.1016/j.trgeo.2025.101555>

Received 31 January 2025; Received in revised form 10 March 2025; Accepted 24 March 2025

Available online 27 March 2025

2214-3912/© 2025 The Author(s). Published by Elsevier Ltd. This is an open access article under the CC BY license (<http://creativecommons.org/licenses/by/4.0/>).

under various factors, including loading magnitude, number of axle load cycles, frequency, confining stress, and other physical state parameters of ballast such as grain shape and size, particle size distribution, mineralogy, moisture content, dry unit weight, and void ratio [20,51,31,53]. Predictive models based on empiricism were developed for BBI based on cyclic deviatoric stress ($q_{cyc,max}$), confining pressure (σ'_3), frequency (f), resilient modulus (M_R) and volumetric strains (ε_v) [31,19,52,24]. These include an empirical relationship proposed by Lackenby et al. [31] relating BBI with $q_{cyc,max}$ and σ'_3 , the volumetric strain-based relationship proposed by Sun et al. [52] and the loading frequency-based relationship proposed by Indraratna et al., [24] and Hussaini and Sweta, [19]. However, the relationship among BBI, M_R and ε_v is elusive because these parameters rely on the $q_{cyc,max}$, σ'_3 , f and ballast gradation, etc. In addition, these empirical relationships were based on statistical regression models, and their application is often confined to the parameters considered during development. As a result, the varying regression parameters in these relationships hinder their applicability across a broader spectrum of loading conditions.

On the other hand, Discrete Element Models (DEM) have been employed to simulate particle breakage under different loading conditions [39,35]. While DEM modelling offers the capability to represent particle breakage through broken bonds, this approach presents a significant hurdle in directly quantifying BBI. Further, owing to the high computational time required for simulating a large number of loading cycles, the prediction of particle breakage becomes inaccurate. Alternatively, constitutive models developed based on fundamental mathematical relationships are also available to predict the breakage of ballast under cyclic loading [45,33]. Though these models effectively capture the stress-strain behaviour, they lack the accuracy of predicting breakage under the large number of load cycles and for different ballast gradations. In addition, determining some model parameters for these constitutive models often involves empiricism, and implementing these models into practice requires sound domain knowledge.

In view of the above-described impediments and challenges, this study delves into the application of machine learning (ML) models for the first time to predict the evolution of ballast degradation with repeated loading. Trained with a wide range of loading and material characteristics, ML models can learn the complex relationships within datasets, while also providing a simple tool that can be used by practising engineers. ML using Artificial Neural Networks (ANN) were earlier used for railway ballast to predict its stress-strain and resilient behaviour under static and cyclic loading [48,21]. ANNs with their ability to effectively model the complex, nonlinear relationships commonly observed in geotechnical materials are widely used by several researchers [48,40,4]. Nonetheless, ANN models are prone to overfitting, particularly when dealing with smaller datasets that are often encountered for particle breakage. In this respect, the current analysis represents an innovative hybrid ML model where a Genetic Algorithm (GA) is used in conjunction with ANN framework to overcome the limitations of traditional ANN approaches. This study differentiates itself from many other ML applications in geotechnical engineering by upholding and validating where warranted, the fundamental geotechnical principles pertinent to BBI prediction. Furthermore, the incorporation of k-fold cross-validation and regularization strengthens the novelty within the framework for BBI prediction, thus providing a simple yet robust alternative to discrete element approaches and traditional constitutive models. Also, by leveraging domain-driven knowledge for input parameter selection, this study distinguishes itself from most “black-box” type ML approaches. The model development presented in this paper follows a four-pronged approach including: (i) development of a Genetic Algorithm-Artificial Neural Network (GA-ANN) model leveraging an existing database; (ii) rigorous model verification with fundamental geotechnical principles and validation using independent laboratory and field database; (iii) comparison of the GA-ANN model with single-objective empirical models, nonlinear regression and other

ML techniques such as support vector machines (SVM) and random forest (RF); and (iv) identification of critical parameters influencing BBI.

Parameter selection for the model

To select the most appropriate parameters for the GA-ANN model, a review of past experimental investigations using large-scale cyclic triaxial and cubical triaxial apparatus was conducted, where several influential parameters indicating the loading characteristics, properties of the granular fabric and its current physical state were identified. Unlike conventional input selection methods such as dimension reduction or filter-based techniques commonly used in the field of machine learning, this study adopts a novel and methodical approach to select inputs based on domain-driven understanding of the mechanism of ballast breakage under cyclic loading. Indraratna et al. [23], through laboratory testing, showed that σ'_3 significantly influenced BBI and proposed an optimal confinement range where breakage is minimal. Below this range, breakage was found to be higher due to the attrition of angular corners, while any increase in σ'_3 beyond the range increased breakage due to particle splitting and crushing. In addition, higher $q_{cyc,max}$ and f accelerate breakage due to a higher amount of kinetic energy being imparted to the granular matrix [53,37]. Further, under prolonged loading, it is observed by several studies [18,27,11] that BBI increases rapidly in the initial loading cycles and slowly reaches a stable state afterwards, albeit depending on the magnitude of three loading parameters (σ'_3 , $q_{cyc,max}$ and f).

Moreover, the initial density of ballast also affects the evolution of breakage [47,56]. A well-graded ballast was reported to degrade less than a uniformly graded ballast, due to the better interlocking effect between particles [55]. Also, ballast with larger maximum and median particle size tends to exhibit greater BBI, due to the susceptibility of larger aggregates to split under stress concentration and corner breakage. To consider these effects, two key parameters characterising the particle size distribution of ballast such as median particle size (D_{50}) and coefficient of uniformity (C_u) were used as inputs in this study. In addition, McDowell and Bolton [34] reported that ballast aggregates with high angularity tend to break more than rounded particles. This effect of angularity on BBI is indirectly accounted for in this study by considering the peak shear strength of ballast (ϕ'_p) as an input parameter. Furthermore, to consider the influence of the initial packing of ballast, the dry density of ballast (γ_d) was considered as an input. Although a few laboratory & field investigations [22,57] reported the importance of the initial void ratio in affecting breakage, it was not considered in this study as it is not often measured in the field during track construction.

During the preparation of the database, it was observed that some studies investigating breakage under cyclic loading did not report ϕ'_p . During machine learning development, replacing missing values with mean or median values is a common and simple approach. However, it may not be suitable in all scenarios and can introduce bias into the model, particularly when the missing data are not randomly distributed. To address this, a nonlinear empirical relationship (see Eq. (1)) between D_{50} and peak friction angle (ϕ'_p) is developed based on past experimental studies, as illustrated in Fig. 1 and then used as input for the current model.

$$\phi'_p = 35.536e^{0.0101D_{50}}; \text{ s.t. } 20 \text{ mm} \leq D_{50} \leq 60 \text{ mm} \quad (1)$$

Moreover, it is to be noted that the mineral composition, surface roughness, particle shape and size of ballast affect the grain-to-grain interaction and, therefore breakage [35,16,15]. While the compressive strength of the parent rock type can influence particle breakage under cyclic loading, it was not considered as an input parameter in this study due to limited data available for training. Previous studies have addressed these aspects; for instance, Asadi et al. [6] focused on predicting abrasive resistance, while Koohmishi and Guo [29] examined

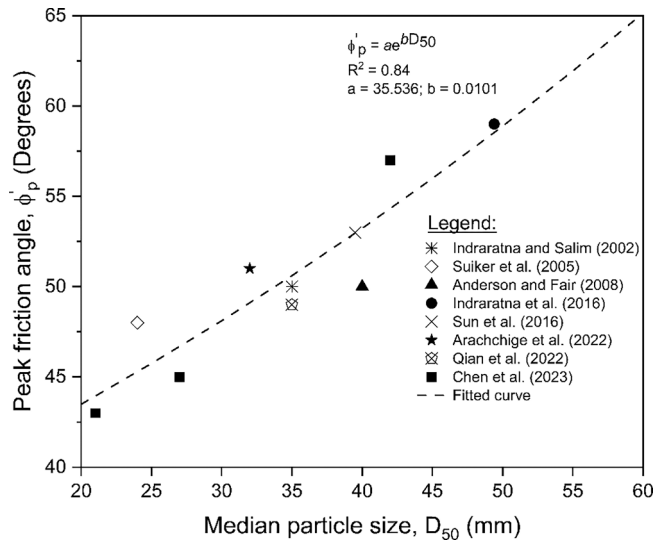


Fig. 1. Relationship between D_{50} and peak friction angle (ϕ'_p) [10,42].

particle breakage under impact loading. The present database considered only data related to fresh ballast material quarried from latite basalt as parent rock.

Based on the aforementioned review of influencing parameters, a total of 8 numeric parameters (N , σ'_3 , $q_{cyc,max}$, f , D_{50} , C_u , γ_d , ϕ'_p) are considered as inputs based on 130 datasets where large-scale cylindrical triaxial or track process simulation apparatus (TPSA) was employed. Large-scale cylindrical triaxial apparatus simulates isotropic compression whereas TPSA accurately replicates the actual stress state in a railway track under plane strain conditions. The ranges of input parameters used in this study are shown in Table 1. An important observation during the database collection was that the magnitude of BBI is affected by the type of apparatus, although the loading conditions were similar. For instance, the results from TPSA yield BBI, on average, 50 % higher than those from the cylindrical triaxial apparatus (Refer to Fig. 2). This was due to plane strain and axisymmetric stress boundary conditions in TPSA and cylindrical triaxial apparatus, respectively. Hence, to address the effect of the testing apparatus, the type of test apparatus was considered as a binary input besides the eight geotechnical parameters, where '1' and '0' represent the data from cylindrical triaxial apparatus and TPSA, respectively. Further, it can be observed from Table 1 that the magnitude of N is in thousands whereas the other parameters are in range of hundreds, hence, natural logarithmic of N was used as an input instead of N , which reduces the risk of overfitting during modelling. Similarly, tangent of peak friction angle ($\tan\phi'_p$) was adopted instead of actual peak friction angle as an input.

During the preparation of datasets, outliers were identified and removed from the database before modelling to avoid inflated errors during the training process. Despite having a lower range for some input

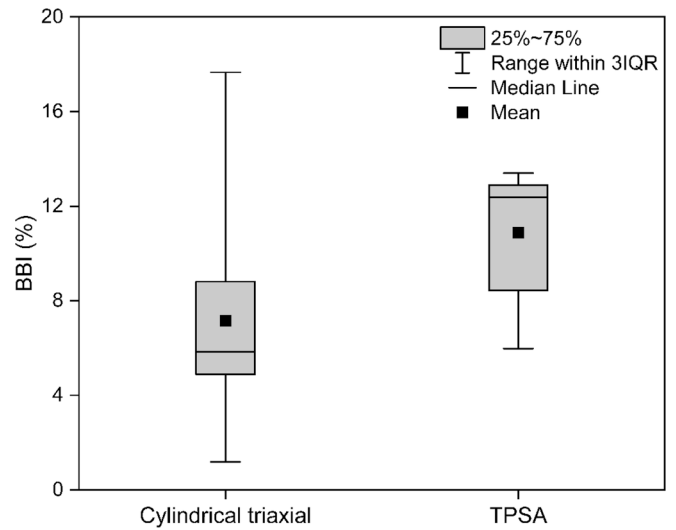


Fig. 2. Variations of measured BBI from different test apparatus.

parameters, it is to be noted that the input parameters considered sufficiently cover a wide range of railway loading conditions observed in the field. For example, C_u varies between 1.2 and 4.5 covering recommended range from most railway standards varying between 1.5 and 2.5 (EN 13450:2002 [9]; CN 12-20C, 2003 [12]; [3]; AS 2758.7: 2015 [5]; [44]). Likewise, cyclic deviatoric stress ranging between 230 and 460 kPa is equivalent to 25 and 45 tonnes axle load and frequency varying from 5 to 60 Hz represents the train speeds from 40 to 400 km/h.

Modelling process

ANN models replicate nonlinear interactions between input and output layers through interconnected nodes and multiple hidden layers. The GA-ANN modelling process is very similar to a conventional ANN model, with the addition of a genetic algorithm that is effectively used to optimise the connection weights between the ANN nodes in each layer. Fig. 3 depicts the three-layer ANN architecture adopted in this study. Only one hidden layer was considered to mitigate the overfitting problem and network complexity, which often arises when multiple hidden layers were used. Additionally, GA was employed in this study to divide the datasets into training and testing subsets, minimising statistical differences and enhancing model performance[8].

To ensure the model robustness and reliability, the dataset was partitioned into training (80 %) and testing (20 %) sets. Systematic partitioning was adopted as suggested by previous studies[49]. Fig. 4 shows the histogram of inputs for training and testing datasets obtained using GA. After data partitioning, the dataset was normalised to a range of -1 to 1 to improve generalisation and ensure consistent input scales. This normalisation was achieved using the following equation:

Table 1
Statistical information of the parameters used in the present study.

Parameter	Cyclic triaxial tests				TPSA tests			
	Min	Max	Mean	SD	Min	Max	Mean	SD
N	1000	500,000	428,247	159,338	10,000	500,000	310,909	182,917
σ'_3 (kPa)	10	240	60.5	58.7	7	15	9.4	3.7
$q_{cyc,max}$ (kPa)	230	500	277.7	95.9	230	460	398.5	97.5
f (Hz)	5	60	21.2	10.9	15	25	16.1	2.7
D_{50} (mm)	27.2	49.4	38.6	3.4	33.5	43	35.6	2.4
C_u	1.2	4	1.8	0.6	1.6	2.5	1.7	0.3
γ_d (kN/m ³)	15.1	16	15.5	0.2	15.3	15.8	15.3	0.1
ϕ'_p (degrees)	44.5	59.5	52.2	2.3	48.7	55.1	50.1	1.6
BBI (%)	1.2	17.7	7.1	3.5	6	13.4	10.9	2.7

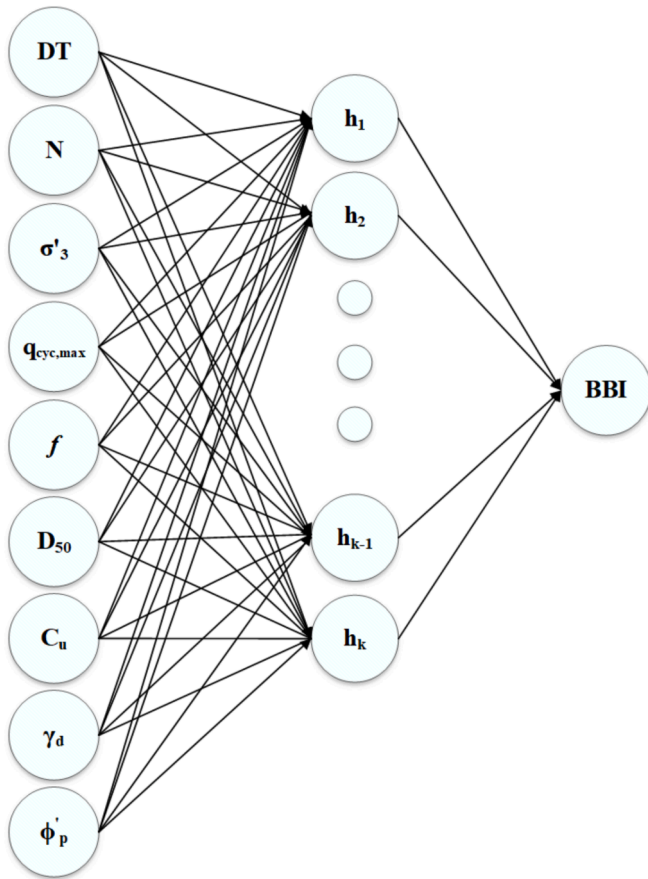


Fig. 3. ANN architecture showing inputs with one hidden layer for BBI prediction.

$$I_{norm} = \frac{2 \times (I - I_{min})}{(I_{max} - I_{min})} - 1 \quad (2)$$

where I_{min} and I_{max} are the minimum and maximum of each parameter, respectively; I_{norm} is the normalised form of parameter.

This present methodology adopts a novel approach by integrating k-fold cross-validation and L2 (Ridge) regularization within the GA-ANN framework, differentiating it from previous GA-ANN approaches. These techniques enhance the generalization capability of hybrid GA-ANN model, particularly when dealing with limited datasets, and effectively prevent overfitting by regulating excessive weights. For the present study, 10-fold (i.e., $k = 10$) cross-validation is adopted to minimise bias during training, ensuring comprehensive utilization of datasets during training. As shown in Fig. 5, the training dataset is divided into 10 folds, where 9 folds are considered for training followed by cross validation with the remaining fold. This process is repeated for all combinations of the 10 folds, and the combination with minimum validation error is selected and used for testing phase. Prior to modelling, the key modelling parameters for both the GA and ANN components were carefully selected. For the GA, parameters such as encoding, crossover and mutation probabilities, termination criteria, selection method, and population size were considered. Likewise, for ANN, the number of hidden nodes, transfer functions, and regularisation technique needed to be initialised (Fig. 5). A real-coded encoding scheme was adopted to represent individuals in the GA population, as the main aim of GA is to optimise ANN weights and biases. Single-point crossover and bit-wise mutation were chosen with probabilities of 0.95 and 0.05, respectively (Cui & Cheng, 2005; Khandelwal et al., 2018; Momeni et al., 2014), while tournament selection was used as the selection method due to its balance between exploration and exploitation. The

mean squared error (MSE) between predicted and measured BBI values was used as the objective function to evaluate model performance. A maximum of 500 iterations and an error tolerance (ϵ) of 0.01 were set as termination criteria to ensure efficient and accurate solutions. While other parameters in GA were kept constant, a parametric study was conducted to determine the optimal population size, which can significantly impact the diversity of potential solutions and the likelihood of finding a global optimum. A logistic (sigmoid) function was applied between the input and hidden layers, while a linear function was used between the hidden and output layers. The integration of L2 (Ridge) regularisation technique with a fixed penalty (λ) term of 0.01 within the GA-ANN model prevents overfitting by constraining the weights, thus preventing no single input parameter disproportionately dominating the predictions. Additionally, the number of hidden nodes in the hidden layer was optimised by varying it from 1 to 20, following previous research [28,58,17]. The flow chart in Fig. 5 illustrates the entire process of the GA-ANN implemented for optimising ANN weights by reducing errors between the experimental and measured BBI.

Performance assessment

The assessment of GA-ANN model developed in this study was conducted in three stages: training and testing and independent validation. In the training and testing stage, the model's capability to understand the intrinsic data relationships within the trained datasets was checked; the external validation stage involved its performance evaluation with unseen datasets; and finally, the verification stage highlighted the advantages of the model when compared against predefined statistical indices. To quantitatively evaluate the performance, 5 metrics were used including root mean square error (RMSE), mean absolute percentage error (MAPE), coefficient of determination (R^2), variance account for (VAF) and A_{20} based following Eqns (3–7)

$$RMSE = \sqrt{\frac{1}{n} \sum_{i=1}^n (BBI_p - BBI_m)^2} \quad (3)$$

$$MAPE = \frac{100}{n} \sum_{i=1}^n \frac{|BBI_p - BBI_m|}{BBI_p} \quad (4)$$

$$R^2 = 1 - \frac{\sum_{i=1}^n (BBI_p - BBI_m)^2}{\sum_{i=1}^n (\overline{BBI}_m - BBI_m)^2} \quad (5)$$

$$VAF = 1 - \left[\frac{\text{var}(BBI_m - BBI_p)}{\text{var}(BBI_m)} \right] * 100 \quad (6)$$

$$A_{20} = \frac{m_{20}}{n} \quad (7)$$

where n is the number of observations; BBI_p , BBI_m and \overline{BBI}_m are the predicted, measured and mean value of BBI, respectively; A_{20} index indicates the predicted observations within 20 % deviation from its original value where m_{20} denotes the number of data points in the range between 0.8 and 1.2 times the measured BBI. For an ideal model, RMSE and MAPE should be zero while R^2 , VAF and A_{20} equals to one.

Training and testing phases

The hybrid GA-ANN model was rigorously evaluated using both training and testing datasets, and performance metrics (Eqns 3–7) were employed to assess the model's accuracy. Notably, the study highlights the impact of population size on model performance, demonstrating that the objective function converged after 250 iterations across all population sizes. This finding warranted the model's ability and effectiveness in achieving optimised convergence during training (Fig. 6). The systematic evaluation of population size underscores the GA-ANN framework's

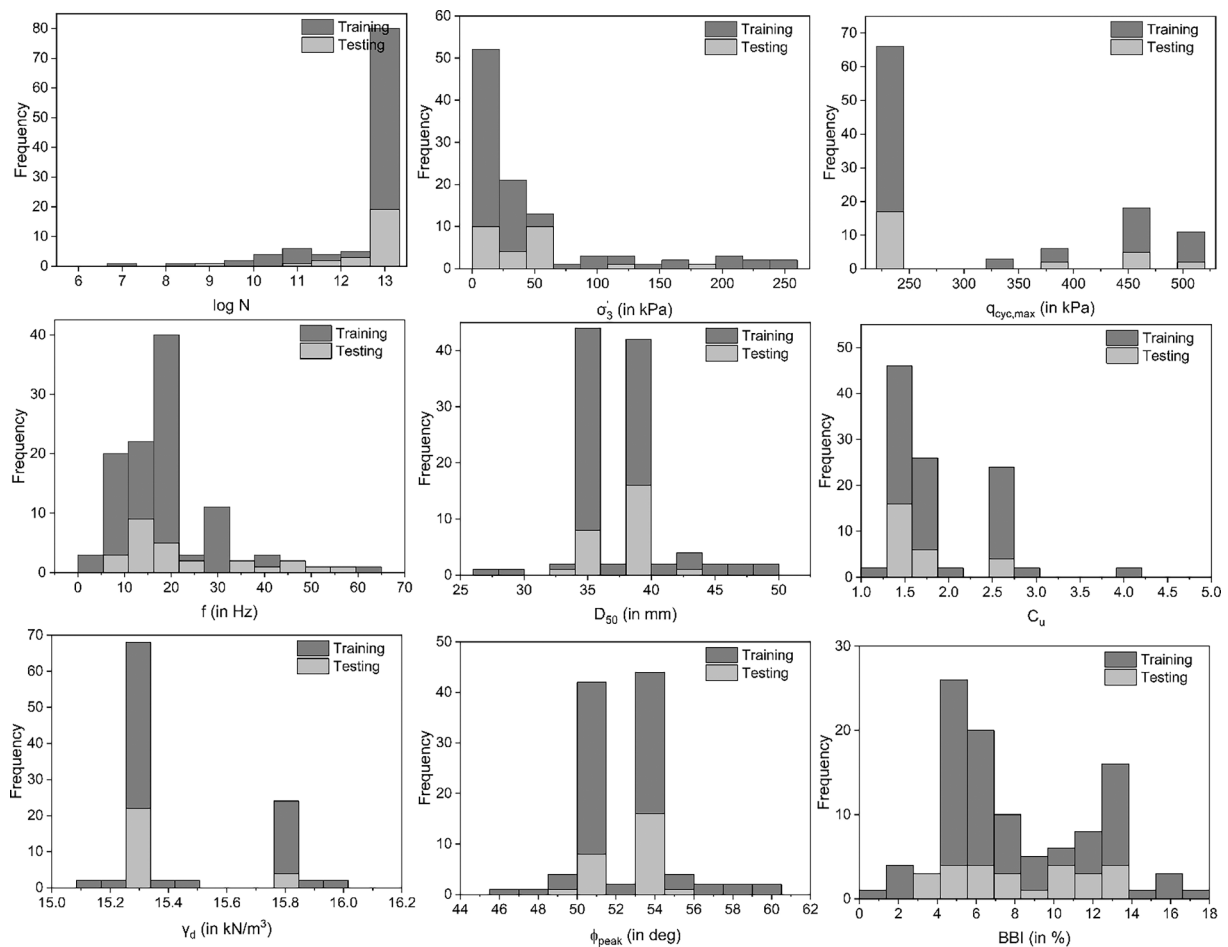


Fig. 4. Histogram plots of data used for training and testing.

reliability, providing key insights for fine-tuning critical GA parameters to enhance prediction of BBI under cyclic loading. While the model with a population size of 500 (model no. 9) exhibited the lowest training error (Table 2), this did not imply that model 9 was the best in optimising the parameters. All models demonstrated promising performance during training, but their true efficacy lied in their ability to generalise unseen (testing) data. To identify the best model in both training and testing phases, a simple ranking procedure proposed by Zorlu et al. [60] was used to select the best-performing model based on the combined scores of these metrics. By considering the performance metrics from both training and testing phases, model no. 6, with a population size of 350, achieved the highest test score and ranked the highest based on its overall score, emerged as the clear frontrunner, demonstrating exceptional performance in both domains (Table 2).

Fig. 7 show the variation of predicted BBI against experimentally measured BBI for training and testing data of model no. 6. With R^2 values consistently exceeding 0.97, the model demonstrates high predictive accuracy and captures a high degree of variance in the BBI data. Furthermore, during the testing phase, the relative deviations between measured and predicted BBI is less than 6 %, while at 88 % of all instances, the predictions are within 20 % deviations. Likewise, $RMSE$ of 0.65 and VAF of 96.9 % indicates the model able to capture underlying trends and variability in BBI prediction. These low $RMSE$, $MAPE$ and high R^2 , VAF and A_{20} metrics prove that the GA-ANN model effectively mitigates bias while being robust to outliers, which highlights the advantages of this model in estimating particle breakage in railway tracks.

Independent Validation

While the performance of the hybrid GA-ANN model appears satisfactory during the training and testing phases, it is essential to evaluate its generalisation capabilities beyond these datasets. Although, the testing data represents the training population, a comprehensive assessment against external data from other studies provides robust and model's predictive abilities. This helps to assess the model's potential to perform well under diverse conditions and avoid overfitting, thereby ensuring its reliability in real-field scenarios. For validation, 33 new independent datasets were collected from similar large-scale experimental setups, encompassing ballast samples predominantly composed of latite basalt and other parent rock types such as dolomite, quartzite, granite and limestone. Furthermore, to evaluate the effectiveness of the hybrid GA-ANN model, its performance was compared against a simple back-propagation ANN. Both the models employed identical hyper-parameters and computational procedures except training methods, k-fold and regularization. The back-propagation ANN used Levenberg-Marquardt training algorithm, while the GA-ANN model utilised the genetic algorithm in optimising network connection weights. Although rigorous analysis was conducted to select the superior ANN model through trial and error, this process was not included in this study as it is beyond the scope of this work. Fig. 8 shows the measured and predicted BBI for the external dataset for both models. The prediction accuracy of GA-ANN model is better than the back-propagation ANN, which demonstrates superior prediction capability and less relative error reduction, whereas GA-ANN model performs well in all five metrics. This superior performance could be attributed to GA's ability to tune the network weights and biases, thereby avoiding local minima.

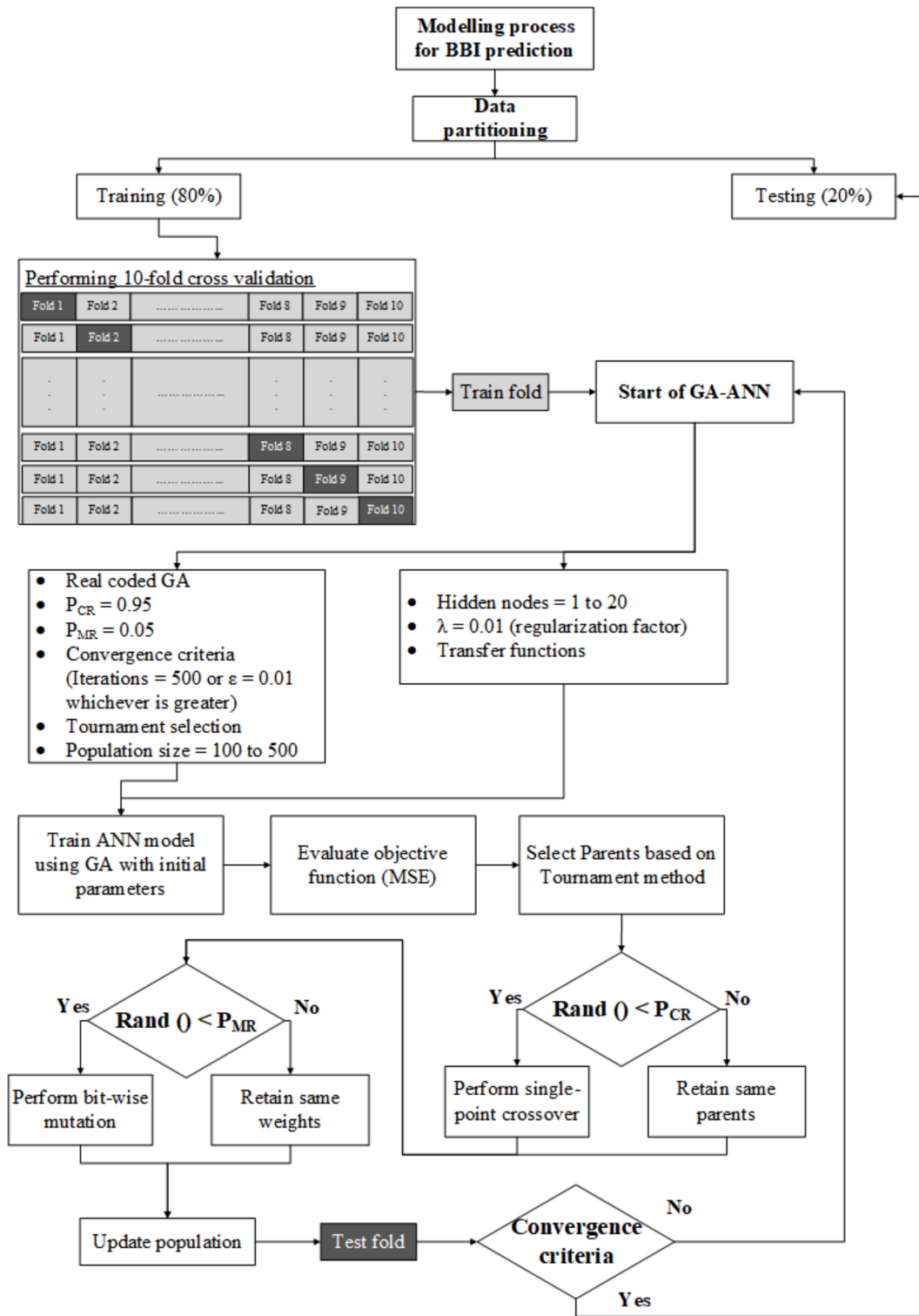


Fig. 5. Flowchart of GA-ANN model adopted for present study.

Further, the proposed hybrid GA-ANN model was compared with BBI, where the data was collected from two independent studies: a railway track in Singleton, New South Wales, Australia [38] and a full-scale track testing facility [14]. Mixed loading conditions with different combinations of axle loads and train speeds, specified by Gu et al. [14] were considered for predicting BBI from the full-scale track testing. However, for predicting field data from Nimbalkar and Indrathna [38], uniform loading conditions with 30 tonnes axle load trains

travelling at an average speed of 80 km/h were assumed as these tracks were predominantly used by heavy-haul trains for transporting iron-ore. By simulating both uniform and mixed traffic conditions, the adaptability of the proposed breakage model was investigated, adopting the input parameters from the original studies and making reasonable assumptions where necessary to ensure accurate representation. The input parameters used for both cases is listed in Table 3.

Fig. 9 illustrates the evolution of breakage under uniform and mixed

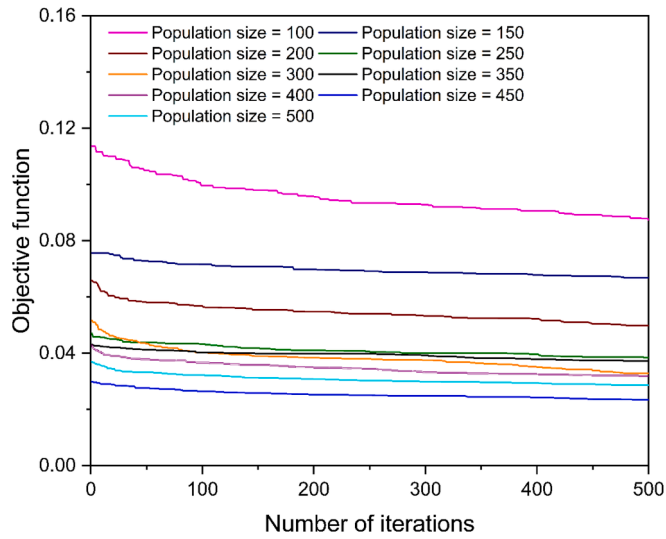


Fig. 6. Effect of population size on the performance of GA-ANN models.

traffic conditions, and the model predictions show its ability to accurately predict the relationship between the number of cycles, cyclic deviatoric stress (i.e., axle load), and frequency (i.e., speed). Although the hybrid GA-ANN model was initially developed based on uniform loading conditions, it effectively generalises to mixed loading scenarios, demonstrating its applicability to diverse real-world traffic conditions with a prediction error of less than 15 %. With real-time data on loading and traffic conditions, the model predictions can provide valuable insights to railway engineers and infrastructure owners, aiding in informed maintenance decisions and ensuring the long-term reliability of railway tracks.

Compliance with geotechnical principles

Though the proposed hybrid GA-ANN model performs well with different datasets, examining its compliance with the prior geotechnical knowledge established after several years of laboratory and field testing is necessary. Such comparisons are essential to ensure the ML model’s reliability when applied to practical scenarios. In this regard, the model was used to predict BBI under scenarios where the stress amplitudes, frequency and gradation conditions under cyclic loading are individually varied and compared against the experimental datasets with similar variations.

Fig. 10 shows the comparison between the experimental data and model predictions. In general, good agreement is observed across different loading and gradation conditions. For example, Fig. 10 (a) shows the evolution of breakage with a number of load cycles (reported by [24]; [25]). The model predictions of BBI up to one million cycles match well with the experimental data, and more importantly, the increase in BBI with increasing q_{cyc} and f is predicted accurately. Fig. 10b shows the model performance on the impact of cyclic deviatoric stress and loading frequency on particle breakage, aligning with previous findings of corner breakage (low level of breakage) at $f < 30$ Hz, and particle splitting and high attrition (high level of breakage) when $30 < f < 60$ Hz. Also, the degradation subjected to compressive forces within the granular assembly is not only due to loading frequency but also due to cyclic deviatoric stress. Similarly, Fig. 10c shows the evolution of ballast breakage at various confining pressures. The model response agrees with the experimental data, which emulates the breakage mechanism of dilation at low confining pressure and particle rolling and sliding at elevated confining pressures and indicates that an optimal confining pressure exists under a given deviatoric stress. Also, the variation of BBI with uniformity coefficient predicted by the model as seen from Fig. 10d captures the reduction of BBI with increasing C_u

Table 2 Performance of GA-ANN models during training and testing stages.

Model no	Population size	Training phase			Testing dataset			Overall score		
		RMSE	MAPE(%)	R^2	RMSE	MAPE(%)	R^2	VAF(%)	A ₂₀	Test score
Performance Metrics	1	0.19	1.47	0.998	1.3	8.7	0.904	86.79	0.885	
	2	0.24	1.95	0.996	1.04	8.78	0.933	92.91	0.731	
	3	0.14	0.77	0.999	1.03	8.98	0.939	93.42	0.731	
	4	0.28	2.41	0.994	0.97	8.09	0.943	93.63	0.846	
	5	0.52	5.2	0.982	0.73	6.41	0.954	95.19	0.962	
	6	0.14	1.36	0.999	0.65	5.95	0.976	96.95	0.885	
	7	0.28	2.37	0.994	0.82	7.39	0.962	95.52	0.885	
	8	0.31	4.06	0.993	0.71	6.92	0.969	96.64	0.808	
	9	0.13	0.81	0.999	0.81	6.99	0.964	96.19	0.846	
Ranking	1	6	6	6	1	3	1	1	4	10
	2	5	5	5	2	2	2	2	1	9
	3	7	9	7	3	1	3	3	1	11
	4	4	3	4	4	4	4	4	3	19
	5	1	1	1	7	8	5	5	5	30
	6	8	7	8	9	9	9	9	4	40
	7	3	4	3	5	5	6	6	4	26
	8	2	2	2	8	7	8	8	2	33
	9	9	8	9	6	6	7	7	3	29

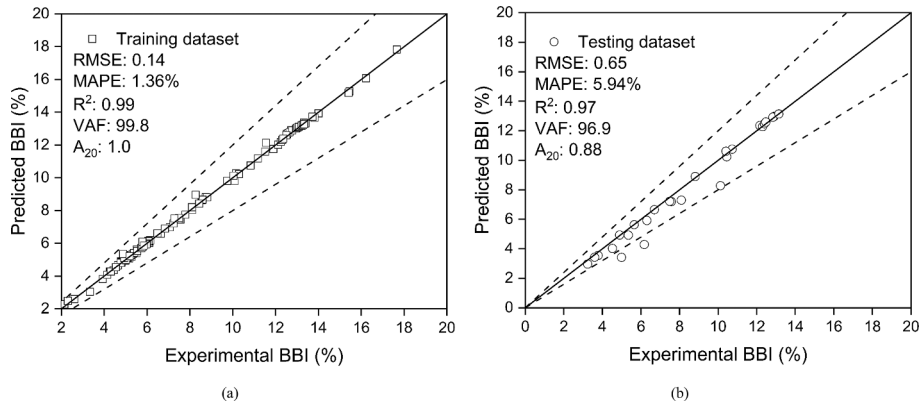


Fig. 7. Regression plots for experimental vs predicted BBI from GA-ANN model (model no.7) (a) Training dataset and (b) Testing dataset [2,7,36,50].

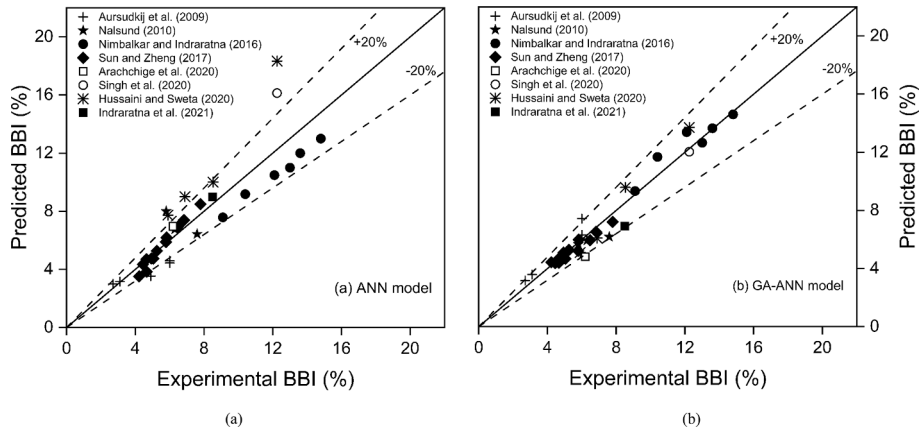


Fig. 8. Experimental vs predicted BBI for external data (a) ANN model (b) GA-ANN model.

Table 3

Input parameters considered for uniform and mixed traffic conditions.

Inputs	Uniform traffic loading [38]	Mixed traffic loading [14]
DT	Considered TPSA boundary condition as like actual railway track	
N	Estimated based on estimated average annual tonnage (Up to 4 million cycles)	Up to 1 million After 200,000 cycles, loading conditions changed
σ_3 (kPa)	10	
$q_{cyc,max}$ (kPa)	$DAF \times Max.Railseatload(Q)$	
	$DAF = 1 + a \left(\frac{V}{D}\right)^\beta$	$DAF = 1 + 0.0052 \frac{V}{D}$
	$Q = \chi \times \frac{A_t}{2} \times 10$	
	Where χ varies from 40 % – 60 % of the static wheel load	
f (Hz)	Equivalent train speed* \approx 80 km/h	Equivalent train speed* \approx 100 to 360 km/h
D_{50} (mm)	35	40.5
C_u	1.6	1.5
γ_d (kN/m ³)	16.5	17.1
ϕ'_p (Deg)	As per Eqn (1)	

DAF: Dynamic amplification factor; V = Train speed (in km/h); D = Diameter of wheel (in m); At: Axle load (in tonnes) B: Width of sleeper (0.26 m); L: Length of sleeper (2.5 m).

*Note: Equivalent cyclic frequency estimated based on characteristic length of the bogie from train speed.

values as observed from laboratory testing, which is due to better interlocking effect (better packing) thus reducing the stress concentration [26,54,55].

Model comparison with empirical and other ML models

Despite extensive research into investigating particle breakage [23,53], there remains a limited number of empirical models to estimate BBI. Only empirical models that utilise the same input parameters were considered to ensure relevance and applicability to this study. Specifically, two widely used equations for BBI in terms of cyclic deviatoric stress [30] and loading frequency [19] were used for comparison.

Lackenby [30]

$$BBI = ce^{(d^{\alpha} q_{cyc,max})} \tag{8}$$

Hussaini and Sweta [19]

$$BBI = me^{(n^{\alpha} f)} \tag{9}$$

In addition to empirical models, machine learning (ML) algorithms namely Support Vector Machines (SVM) and Random Forest (RF) were employed and compared with the proposed GA-ANN model due to their widespread application in geotechnical studies [13,32]. These algorithms were chosen for their ability to handle high nonlinearity and their adaptability, which can enhance computational efficiency. Furthermore, the performance of these ML techniques was compared with traditional nonlinear multivariate regression (MR) models using an external validation database. Although a detailed modelling process was carried out for SVM, RF, and MR including identifying the best model during training and testing phases via a ranking procedure, this detailed process is beyond the scope of the current study.

Fig. 11 illustrates the comparison of two empirical models alongside five machine learning models (MR, SVM, RF, ANN, and GA-ANN) using a spider chart, where the axes represent various performance indicators

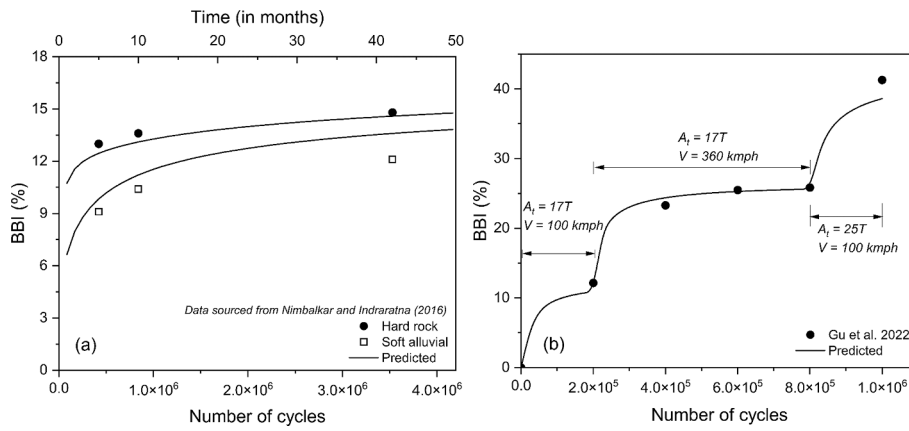


Fig. 9. Validation of the proposed model against (a) uniform loading (b) mixed loading with respect to number of cycles.

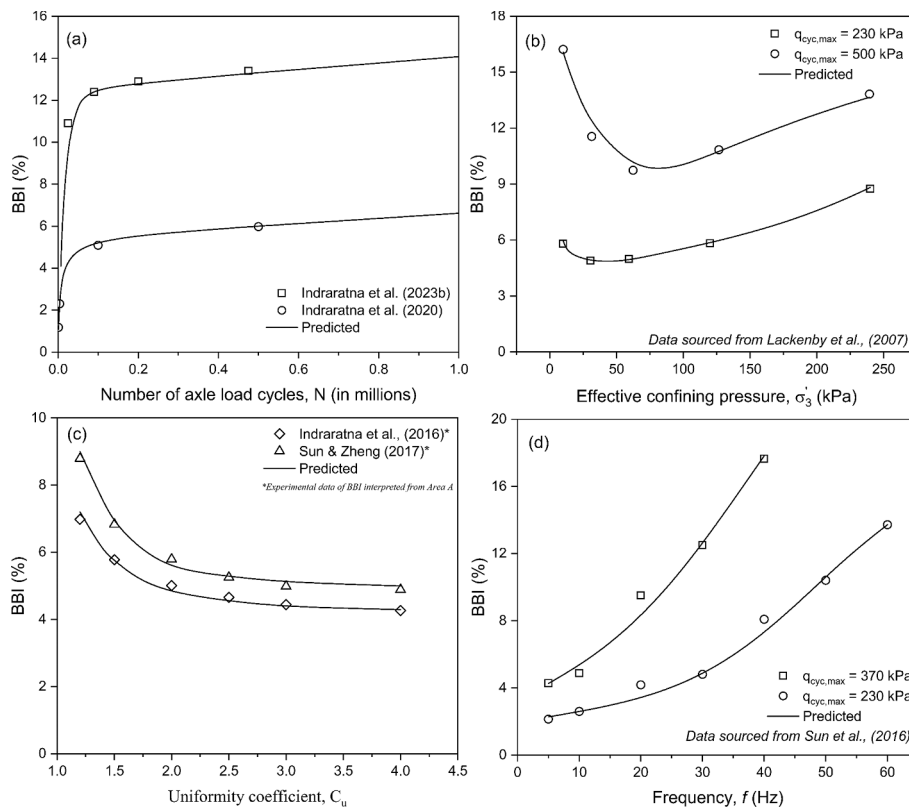


Fig. 10. Model predictions using proposed GA-ANN model.

(Eqns. 3–7). The results indicate that the ML models demonstrate superior predictive capabilities, with the GA-ANN model outperforming the others (Table 4). Although, the empirical models (Eqns. (8) & (9)) demonstrate satisfactory performance within the specific data range that was investigated in their respective studies, their applicability is constrained to this range, which limits their ability to generalise to broader datasets. Consequently, these models may yield significant errors and inaccurate predictions when applied to data points that deviate substantially from the original training data. It is noteworthy that all the ML models (ANN, GA-ANN, SVM, and RF) outperformed the multivariate regression (MR) model, likely due to the latter’s tendency to overfit when handling a large number of input variables. Moreover, MR models rely on predefined mathematical functions, which may not adequately account for complex interactions between variables, as observed in the current dataset [59].

Among the ML techniques, the ANN model exhibited slightly superior performance achieving ($R^2 = 0.78$) compared to SVM ($R^2 = 0.74$) and RF ($R^2 = 0.67$). Notably, the error (RMSE) from the ANN model is 4.5 % and 24 % lower than those from SVM and RF, respectively, while the error from GA-ANN model was reduced by more than 50 % than those from ANN, SVM and RF models. To further elucidate the advantages of GA-ANN, the evolution of BBI against variations in C_u and $q_{cyc,max}$ are plotted in Fig. 12(a) and (b) respectively and compared with predictions from SVM and RF. While RF exhibited low prediction accuracy, SVM predictions closely followed the training data causing overfitting, which compromises reliability on unseen datasets. In contrast, GA-ANN effectively learned the underlying relationships, thus being able to predict the trend with increased reliability and higher accuracy (Fig. 10). Similarly, Fig. 12(c) and (d) demonstrate the performance of SVM and RF models, revealing their limited generalisation

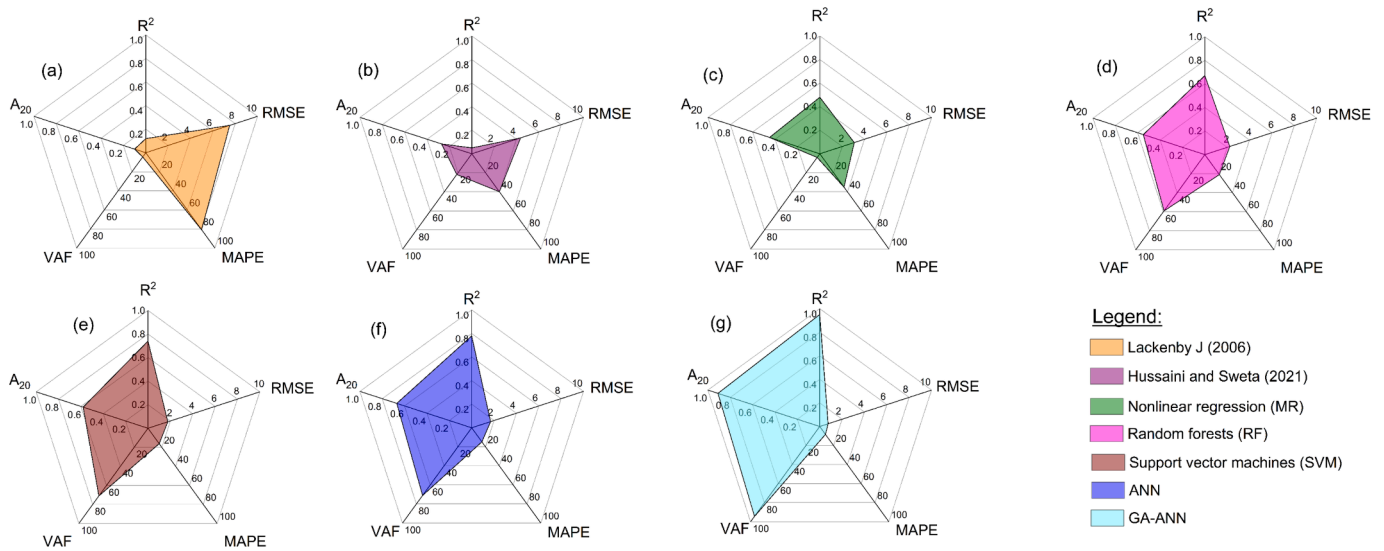


Fig. 11. Spider plots showing performance of different models (a) Eqn (8) (b) Eqn (9) (c) MR (d) RF (e) SVM (f) ANN (g) GA-ANN.

Table 4
Comparison of performance metrics of different models for external dataset.

Model	RMSE	MAPE(%)	R ²	VAF(%)	A ₂₀
Lackenby [30]	7.51	80.8	0.12	4.41	0.10
Hussaini and Sweta [19]	4.37	39.8	0.05	21.6	0.27
MR	3.08	35.0	0.48	3.83	0.45
RF	2.23	21.0	0.67	59.0	0.55
SVM	1.77	16.2	0.74	71.0	0.58
ANN	1.69	14.8	0.78	71.0	0.67
GA-ANN	0.75	8.2	0.95	94.2	0.91

ability and substantially larger deviations from measured BBI when applied to an external validation database. This indicates that, without employing the genetic algorithm, ML models prone to loss of accuracy, potentially leading to convergence to local minima when analysing this specific ballast breakage dataset, as reflected in the R² and RMSE values. Although both SVM and RF adept at handling nonlinear problems, their marginally lower performance can be attributed to several factors: (i) the characteristics of the BBI dataset, which may contain complex, nonlinear relationships better suited to ANN's deep learning capabilities, (ii) SVM's potential limitations in regression tasks, particularly when selecting the appropriate kernel function and scaling for nonlinearity, and (iii) RF's increased computational complexity and

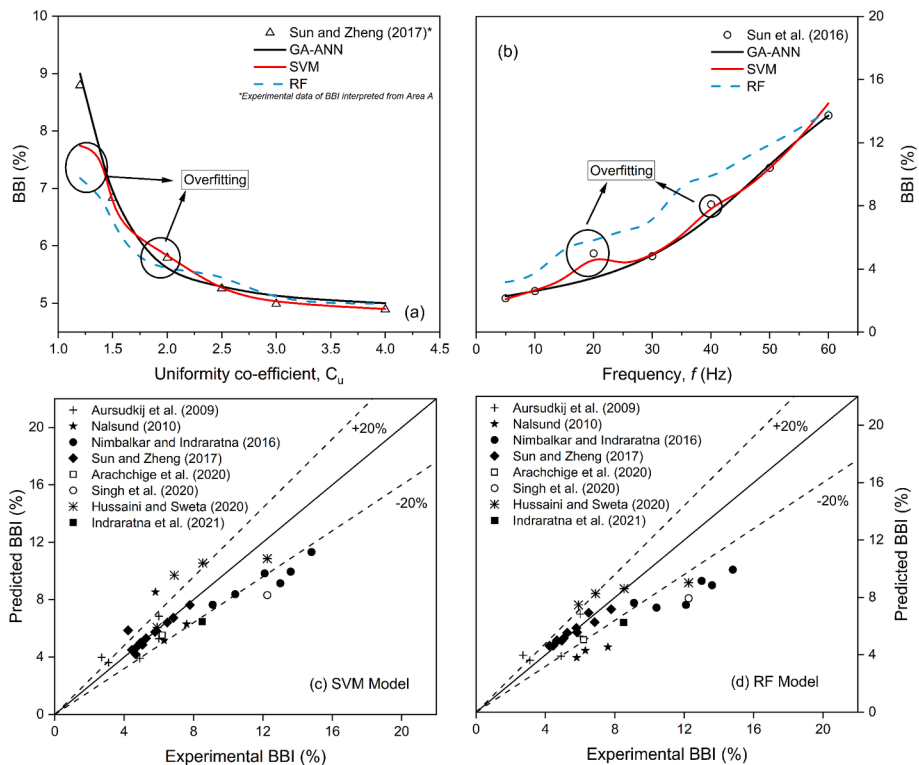


Fig. 12. Prediction of SVM and RF models showing overfitting compared with GA-ANN (a) effect of C_u (b) effect of f and q_{cyc,max}; prediction deviations due to overfitting against external database (c) SVM (d) RF.

interpretability when constructing a large number of trees which could have an impact on its efficiency.

Ultimately, the GA-ANN model achieved high *VAF*, low *RMSE*, and *MAPE* values, thus reflecting its exceptional ability to generalise to unseen data, while *MAPE* and A_{20} evaluates the model's resilience to outliers. Therefore, these characteristics make the GA-ANN model a promising tool for real-time BBI prediction in railway tracks, and it can be integrated into existing railway monitoring systems to enhance the predictive maintenance capabilities.

Sensitivity analysis

Sensitivity analysis was carried out to investigate the relative influence of input parameters on the developed breakage model, as uncertainty associated with the input data can affect the outcomes of the GA-ANN model. Sobol sensitivity analysis was adopted for the present study to quantify the significance of input parameters, including direct and interaction effects on BBI. Sobol indices were estimated using quasi-random Monte-Carlo sampling based on Saltelli et al. [46] to determine the input parameters influencing BBI. Fig. 13 shows the results of Sobol analysis, highlighting the relative influence of input parameters on BBI. The first-order index (S_i) measures the contribution of individual input parameters while the total index (S_{Ti}) depicts both direct and interaction effects with other inputs. Results of Sobol analysis (Fig. 13) indicate that cyclic deviatoric stress ($q_{cyc,max}$) is the most dominant parameter where S_i is greater than 0.28, while the number of cycles (N) and frequency are the next most influential parameters, with both their S_i 's equal to 0.16. However, the interaction index reveals that the number of cycles affects BBI significantly than f , and thus, their order is considered accordingly. Furthermore, it can be observed that the direct effect (S_i) of gradation parameters (D_{50} and C_u) have minimal impact on BBI however, these parameters influence BBI greatly while interacting with other parameters. It is important to note that, the impact of C_u alone did not affect BBI while its interaction affects significantly, where its interaction index is greater than its first order index.

After a thorough analysis of the Sobol results, the input parameters in this study are categorised into three types: (i) primary: parameters with high $S_i \geq 0.1$, (ii) secondary: parameters with small S_i ($0.05 \leq S_i < 0.1$) and high $S_{Ti} \geq 0.05$ and (iii) tertiary: parameters with low $S_i \geq 0$ and $S_{Ti} \geq 0$ [43]. Significant importance should be paid to primary parameters, mainly accounting for variation in breakage ($q_{cyc,max}$, f , N and σ'_3) where its direct impact is more than 10 %, and special attention must be taken

to avoid underestimating the effects of secondary parameters, because their interaction effects have a large contribution to breakage (D_{50} , C_u and ϕ'_p) and dry density is the least important parameter. These findings offer valuable guidance on the response of particle breakage, including external loads, ballast gradation, and particle angularity.

Limitations

While the proposed hybrid GA-ANN model demonstrated superior predictive capability in estimating ballast breakage under cyclic loading, the following limitations should be considered when evaluating its applicability beyond the specific conditions of this study.

- The GA-ANN model developed in this study to predict BBI under cyclic loading conditions was based on the available data on fresh ballast and predominantly basalt being the parent rock type. Though the model has good predictive ability, caution must be exercised while extending this model to other parent rock types.
- Material properties such as the strength of the parent rock, particle characteristics such as ballast shape and size, parameters including surface roughness, flakiness, elongation, sphericity were not considered due to data unavailability. Additionally, the effects of weathering, environmental conditions and tamping operations were not considered in the present study owing to unavailability of sufficient information.
- The hybrid GA-ANN model was developed based on large-scale laboratory experimental conditions; hence this model cannot envisage BBI under principal stress rotation [41,33].

Conclusions

This paper presents a novel prediction model to determine the particle breakage of ballast under varied cyclic loading conditions using a hybrid GA-ANN framework. A key highlight of this framework is the integration of k-fold validation, which distinguishes it from traditional ML models by effectively addressing the challenges of limited datasets encountered with BBI. The proposed GA-ANN model was able to capture the evolution of breakage with all input parameters N , σ'_3 , $q_{cyc,max}$, f , D_{50} , C_u , γ_d and ϕ'_p that commonly affect ballast degradation in railway tracks. Based on rigorous analysis of model performance, the following specific conclusions can be made:

1. The proposed hybrid GA-ANN model predicted the evolution of ballast breakage under various loading conditions in the laboratory with very high accuracy, yielding R^2 , *MAPE* and *RMSE* of 0.95, 8.23 % and 0.75, respectively. This underscores that the proposed model effectively captures the influence of all key parameters, thus providing a reliable tool for assessing ballast degradation.
2. The hybrid GA-ANN model, meticulously tuned for optimal weights, biases, and hidden node configurations through advanced regularization techniques, outperformed ANN, SVM, RF, MR and empirical models in predicting ballast breakage. More importantly, for unseen datasets, GA-ANN yielded an R^2 of 0.95, while R^2 of 0.78, 0.74, 0.67 and 0.48 were obtained for ANN, SVM, RF and MR, respectively. The inclusion of regularization, in this GA-ANN framework, effectively mitigates overfitting, a limitation in existing models, further enhancing its robustness. This highlights that the proposed GA-ANN model is more rigorous and possesses superior capability in accurately predicting BBI from sources external to its training dataset, making it more viable for application in practice.
3. The proposed hybrid GA-ANN model exhibits high predictive accuracy and aligns with geotechnical fundamentals governing particle breakage mechanisms under cyclic loading. Notably, the model demonstrates reliable performance under varying conditions, including high axle loads, diverse train speeds, and different ballast

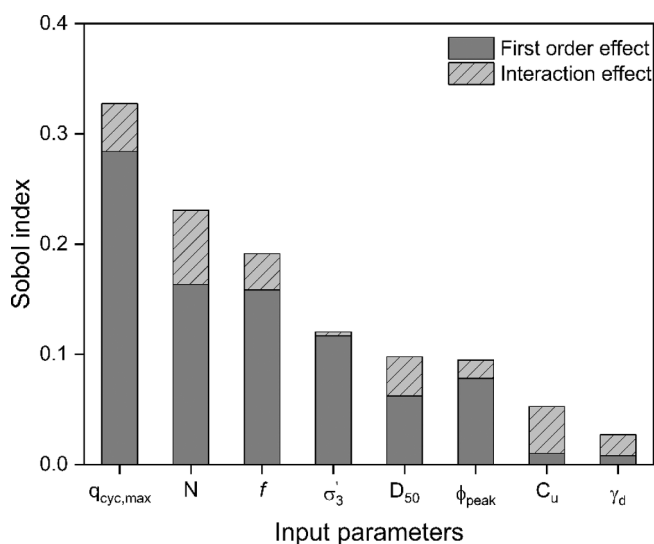


Fig. 13. Results of global sensitivity analysis showing Sobol indices for breakage model.

particle size distributions, further solidifying its superiority over existing models and thus reinforcing its practical applicability to ballasted railway tracks

- The use of boundary conditions of the test set up as a binary input improved the model's training process to distinguish laboratory and field conditions, leading to more accurate predictions of breakage with < 15 % error for the Singleton railway track. Moreover, the model's ability to simulate breakage under mixed traffic conditions (i.e., diverse train speed and axle load combinations) further solidifies its versatility and applicability to various practical scenarios.
- Based on Sobol analysis, cyclic deviatoric stress, number of cycles, and frequency are identified as the primary input parameters that highly influence BBI, followed by gradation parameters classified as secondary inputs. This classification of input parameters will enable practising engineers to prioritise maintenance operations and allocate resources effectively to mitigate breakage and ensure the long-term reliability of railway tracks.

CRedit authorship contribution statement

Srinivas Alagesan: Writing – review & editing, Writing – original draft, Methodology, Investigation, Formal analysis, Data curation, Conceptualization. **Buddhima Indraratna:** Writing – review & editing, Visualization, Validation, Supervision, Software, Resources, Project administration, Methodology, Investigation, Funding acquisition, Conceptualization. **Rakesh Sai Malisetty:** Writing – review & editing, Visualization, Validation, Methodology, Formal analysis. **Yujie Qi:** Writing – review & editing, Supervision, Project administration, Methodology, Investigation, Conceptualization. **Cholachat Rujikiatkamjorn:** Writing – review & editing, Visualization, Supervision, Project administration.

Declaration of competing interest

The authors declare that they have no known competing financial interests or personal relationships that could have appeared to influence the work reported in this paper.

Acknowledgements

The authors are grateful for the financial support from the Australian Research Council (ARC-LP200200915) and acknowledge the financial and technical support from industry partners including Sydney Trains, Australian Rail Transport Corporation (ARTC), SMEC Australia Pty. Limited, Bentley Systems Pty. Limited, and Bestech Australia Pty. Limited.

Data availability

Data will be made available on request.

References

- Anderson WF, Fair P. Behavior of Railroad Ballast under Monotonic and Cyclic Loading. *Journal of Geotechnical and Geoenvironmental Engineering* 2008;134(3): 316–27. [https://doi.org/10.1061/\(ASCE\)1090-0241\(2008\)134:3\(316\)](https://doi.org/10.1061/(ASCE)1090-0241(2008)134:3(316)).
- Arachchige CMK, Indraratna B, Qi Y, Vinod JS, Rujikiatkamjorn C. Deformation and degradation behaviour of Rubber Intermixed Ballast System under cyclic loading. *Eng Geol* 2022;307:106786. <https://doi.org/10.1016/j.enggeo.2022.106786>.
- AREMA, 2010. Manual for Railway Engineering. American Railway Engineering and Maintenance-of-way Association, Maryland, USA.
- Armaghani DJ, Hajihassani M, Mohamad ET, Marto A, Noorani SA. Blasting-induced flyrock and ground vibration prediction through an expert artificial neural network based on particle swarm optimisation. *Arab J Geosci* 2014;7(12):5383–96. <https://doi.org/10.1007/s12517-013-1174-0>.
- AS (Australian Standards), 2015. Aggregates and rock for engineering purposes. Part 7: Railway ballast AS 2758.7, Standards Australia.
- Asadi M, Taghavi Ghalesari A, Kumar S. Machine learning techniques for estimation of Los Angeles abrasion value of rock aggregates. *Eur J Environ Civ Eng* 2022;26(3):964–77. <https://doi.org/10.1080/19648189.2019.1690585>.
- Aursudkij B, McDowell GR, Collop AC. Cyclic loading of railway ballast under triaxial conditions and in a railway test facility. *Granul Matter* 2009;11(6):391. <https://doi.org/10.1007/s10035-009-0144-4>.
- Bowden GJ, Maier HR, Dandy GC. Optimal division of data for neural network models in water resources applications. *Water Resour Res* 2002;38(2):2-1-2-11. <https://doi.org/10.1029/2001WR000266>.
- En BS, 13450. Aggregate for Railway Ballast. *British Standards Institution* 2003.
- Chen J, Liu Y, Hu Q, Gao R. Effects of Particle Size and Grading on the Breakage of Railway Ballast. *Laboratory Testing and Numerical Modeling Sustainability* 2023; 15(23). <https://doi.org/10.3390/su152316363>.
- Chen J, Vinod JS, Indraratna B, Ngo NT, Gao R, Liu Y. A discrete element study on the deformation and degradation of coal-fouled ballast. *Acta Geotech* 2022;17(9): 3977–93. <https://doi.org/10.1007/s11440-022-01453-4>.
- CN 12-20 C, 2003. Crushed Rock Ballast. *Canadian National Railways Specification*.
- Ebid AM. 35 Years of (AI) in Geotechnical Engineering: State of the Art. *Geotech Geol Eng* 2021;39(2):637–90. <https://doi.org/10.1007/s10706-020-01536-7>.
- Gu Q, Zhao C, Bian X, Morrissey JP, Ooi JY. Trackbed settlement and associated ballast degradation due to repeated train moving loads. *Soil Dyn Earthq Eng* 2022; 153:107109. <https://doi.org/10.1016/j.soildyn.2021.107109>.
- Guo Y, Xie J, Fan Z, Markine V, Connolly DP, Jing G. Railway ballast material selection and evaluation: A review. *Constr Build Mater* 2022;344:128218. <https://doi.org/10.1016/j.conbuildmat.2022.128218>.
- Gupta A, Madhusudhan BN, Zervos A, Powrie W, Harkness J, Le Pen L. Grain characterisation of fresh and used railway ballast. *Granul Matter* 2022;24(4):96. <https://doi.org/10.1007/s10035-022-01263-1>.
- Hecht-Nielsen, R. (1987, June). Kolmogorov's mapping neural network existence theorem. In Proceedings of the international conference on Neural Networks (Vol. 3, pp. 11-14). New York, NY, USA: IEEE press.
- Hossain Z, Indraratna B, Darve F, Thakur PK. DEM analysis of angular ballast breakage under cyclic loading. *Geomech Geoen* 2007;2(3):175–81. <https://doi.org/10.1080/17486020701474962>.
- Hussaini SKK, Sweta K. Investigation of deformation and degradation response of geogrid-reinforced ballast based on model track tests. Proceedings of the Institution of Mechanical Engineers, Part F: Journal of Rail and Rapid Transit 2020; 235(4):505–17. <https://doi.org/10.1177/0954409720944687>.
- Indraratna, B., & Salim, W. (2002). Modelling of particle breakage of coarse aggregates incorporating strength and dilatancy. Proceedings of the Institution of Civil Engineers - Geotechnical Engineering, 155(4), 243–252. Doi: 10.1680/jeng.2002.155.4.243.
- Indraratna B, Armaghani DJ, Gomes Correia A, Hunt H, Ngo T. Prediction of resilient modulus of ballast under cyclic loading using machine learning techniques. *Transp Geotech* 2023;38:100895. <https://doi.org/10.1016/j.trgeo.2022.100895>.
- Indraratna B, Ionescu D, Christie HD. Shear Behavior of Railway Ballast Based on Large-Scale Triaxial Tests. *Journal of Geotechnical and Geoenvironmental Engineering* 1998;124(5):439–49. [https://doi.org/10.1061/\(ASCE\)1090-0241\(1998\)124:5\(439\)](https://doi.org/10.1061/(ASCE)1090-0241(1998)124:5(439)).
- Indraratna B, Lackenby J, Christie D. Effect of confining pressure on the degradation of ballast under cyclic loading. *Géotechnique* 2005;55(4):325–8. <https://doi.org/10.1680/geot.2005.55.4.325>.
- Indraratna B, Ngo T, Rujikiatkamjorn C. Performance of Ballast Influenced by Deformation and Degradation: Laboratory Testing and Numerical Modeling. *International Journal of Geomechanics* 2020;20(1):04019138. [https://doi.org/10.1061/\(ASCE\)GM.1943-5622.0001515](https://doi.org/10.1061/(ASCE)GM.1943-5622.0001515).
- Indraratna, B., Rujikiatkamjorn, C., & Salim, W. (2023b). Advanced rail geotechnology—ballasted track. 2nd Edition. CRC press.
- Indraratna B, Sun Y, Nimbalkar S. Laboratory Assessment of the Role of Particle Size Distribution on the Deformation and Degradation of Ballast under Cyclic Loading. *Journal of Geotechnical and Geoenvironmental Engineering* 2016;142(7): 04016016. [https://doi.org/10.1061/\(ASCE\)GT.1943-5606.0001463](https://doi.org/10.1061/(ASCE)GT.1943-5606.0001463).
- Indraratna B, Thakur PK, Vinod JS. Experimental and Numerical Study of Railway Ballast Behavior under Cyclic Loading. *International Journal of Geomechanics* 2010;10(4):136–44. [https://doi.org/10.1061/\(ASCE\)GM.1943-5622.0000055](https://doi.org/10.1061/(ASCE)GM.1943-5622.0000055).
- Kaastra I, Boyd M. Designing a neural network for forecasting financial and economic time series. *Neurocomputing* 1996;10(3):215–36. [https://doi.org/10.1016/0925-2312\(95\)00039-9](https://doi.org/10.1016/0925-2312(95)00039-9).
- Koohmishi M, Guo Y. Machine learning approach to railway ballast degradation prognosis considering crumb rubber modification and parent rock strength. *Constr Build Mater* 2023;409:133985. <https://doi.org/10.1016/j.conbuildmat.2023.133985>.
- Lackenby J. Triaxial behaviour of ballast and the role of confining pressure under cyclic loading. *Australia: University of Wollongong*; 2006.
- Lackenby J, Indraratna B, McDowell G, Christie D. Effect of confining pressure on ballast degradation and deformation under cyclic triaxial loading. *Géotechnique* 2007;57(6):527–36. <https://doi.org/10.1680/geot.2007.57.6.527>.
- Liu H, Su H, Sun L, Dias-da-Costa D. State-of-the-art review on the use of AI-enhanced computational mechanics in geotechnical engineering. *Artif Intell Rev* 2024;57(8):196. <https://doi.org/10.1007/s10462-024-10836-w>.
- Malisetty RS, Indraratna B, Vinod J. Behaviour of ballast under principal stress rotation: Multi-laminate approach for moving loads. *Comput Geotech* 2020;125: 103655. <https://doi.org/10.1016/j.compgeo.2020.103655>.

- [34] McDowell GR, Bolton MD. On the micromechanics of crushable aggregates. *Géotechnique* 1998;48(5):667–79. <https://doi.org/10.1680/geot.1998.48.5.667>.
- [35] McDowell GR, Li H. Discrete element modelling of scaled railway ballast under triaxial conditions. *Granul Matter* 2016;18(3):66. <https://doi.org/10.1007/s10035-016-0663-8>.
- [36] Nålund R. Effect of Grading on Degradation of Crushed-Rock Railway Ballast and on Permanent Axial Deformation. *Transp Res Rec* 2010;2154(1):149–55. <https://doi.org/10.3141/2154-15>.
- [37] Ngo T, Indraratna B, Ferreira F. Influence of synthetic inclusions on the degradation and deformation of ballast under heavy-haul cyclic loading. *International Journal of Rail Transportation* 2022;10(4):413–35. <https://doi.org/10.1080/23248378.2021.1964390>.
- [38] Nimbalkar S, Indraratna B. Improved Performance of Ballasted Rail Track Using Geosynthetics and Rubber Shockmat. *Journal of Geotechnical and Geoenvironmental Engineering* 2016;142(8):04016031. [https://doi.org/10.1061/\(ASCE\)GT.1943-5606.0001491](https://doi.org/10.1061/(ASCE)GT.1943-5606.0001491).
- [39] O'Sullivan C, Cui L, O'Neill SC. Discrete element analysis of the response of granular materials during cyclic loading. *SOILS AND FOUNDATIONS* 2008;48(4):511–30. <https://doi.org/10.3208/sandf.48.511>.
- [40] Penumadu D, Zhao R. Triaxial compression behavior of sand and gravel using artificial neural networks (ANN). *Comput Geotech* 1999;24(3):207–30. [https://doi.org/10.1016/S0266-352X\(99\)00002-6](https://doi.org/10.1016/S0266-352X(99)00002-6).
- [41] Powrie W, Yang LA, Clayton CRI. Stress changes in the ground below ballasted railway track during train passage. *Proceedings of the Institution of Mechanical Engineers, Part F: Journal of Rail and Rapid Transit* 2007;221(2):247–62. <https://doi.org/10.1243/0954409JRR95>.
- [42] Qian Y, Tutumluer E, Hashash YMA, Ghaboussi J. Triaxial testing of new and degraded ballast under dry and wet conditions. *Transp Geotech* 2022;34:100744. <https://doi.org/10.1016/j.trgeo.2022.100744>.
- [43] Ratto M, Tarantola S, Saltelli A. Sensitivity analysis in model calibration: GSA-GLUE approach. *Comput Phys Commun* 2001;136(3):212–24. [https://doi.org/10.1016/S0010-4655\(01\)00159-X](https://doi.org/10.1016/S0010-4655(01)00159-X).
- [44] RDSO, 2016. Specification for Track Ballast, Research Designs and Standards Organization, IRS: GE-1. Ministry of Railways, Government of India.
- [45] Salim W, Indraratna B. A new elastoplastic constitutive model for coarse granular aggregates incorporating particle breakage. *Can Geotech J* 2004;41(4):657–71. <https://doi.org/10.1139/t04-025>.
- [46] Saltelli A, Annoni P, Azzini I, Campolongo F, Ratto M, Tarantola S. Variance based sensitivity analysis of model output. Design and estimator for the total sensitivity index. *Comput Phys Commun* 2010;181(2):259–70. <https://doi.org/10.1016/j.cpc.2009.09.018>.
- [47] Selig ET, Waters JM. *Track geotechnology and substructure management*. Thomas Telford; 1994.
- [48] Shahin MA, Indraratna B. Modeling the mechanical behavior of railway ballast using artificial neural networks. *Can Geotech J* 2006;43(11):1144–52. <https://doi.org/10.1139/t06-077>.
- [49] Shahin MA, Maier HR, Jaksa MB. Data Division for Developing Neural Networks Applied to Geotechnical Engineering. *J Comput Civ Eng* 2004;18(2):105–14. [https://doi.org/10.1061/\(ASCE\)0887-3801\(2004\)18:2\(105\)](https://doi.org/10.1061/(ASCE)0887-3801(2004)18:2(105)).
- [50] Singh RP, Nimbalkar S, Singh S, Choudhury D. Field assessment of railway ballast degradation and mitigation using geotextile. *Geotext Geomembr* 2020;48(3):275–83. <https://doi.org/10.1016/j.geotexmem.2019.11.013>.
- [51] Suiker AS, Selig ET, Frenkel R. Static and Cyclic Triaxial Testing of Ballast and Subballast. *Journal of Geotechnical and Geoenvironmental Engineering* 2005;131(6):771–82. [https://doi.org/10.1061/\(ASCE\)1090-0241\(2005\)131:6\(771\)](https://doi.org/10.1061/(ASCE)1090-0241(2005)131:6(771)).
- [52] Sun QD, Indraratna B, Nimbalkar S. Effect of cyclic loading frequency on the permanent deformation and degradation of railway ballast. *Géotechnique* 2014;64(9):746–51. <https://doi.org/10.1680/geot.14.T.015>.
- [53] Sun QD, Indraratna B, Nimbalkar S. Deformation and Degradation Mechanisms of Railway Ballast under High Frequency Cyclic Loading. *Journal of Geotechnical and Geoenvironmental Engineering* 2016;142(1):04015056. [https://doi.org/10.1061/\(ASCE\)GT.1943-5606.0001375](https://doi.org/10.1061/(ASCE)GT.1943-5606.0001375).
- [54] Sun Y, Zheng C. Breakage and shape analysis of ballast aggregates with different size distributions. *Particuology* 2017;35:84–92. <https://doi.org/10.1016/j.partic.2017.02.004>.
- [55] Sun Y, Nimbalkar S, Chen C. Grading and frequency dependence of the resilient modulus of ballast. *Géotechnique Letters* 2018;8(4):305–9. <https://doi.org/10.1680/jgele.18.00084>.
- [56] Tutumluer E, Huang H, Hashash Y, Ghaboussi J. (September). Aggregate shape effects on ballast tamping and railroad track lateral stability. In: *In Proceedings of the AREMA Annual conference*; 2006. p. 17–20.
- [57] Tutumluer E, Qian Y, Hashash YMA, Ghaboussi J, Davis DD. Discrete element modelling of ballasted track deformation behaviour. *International Journal of Rail Transportation* 2013;1(1–2):57–73. <https://doi.org/10.1080/23248378.2013.788361>.
- [58] Wang C. *A theory of generalisation in learning machines with neural network applications*. University of 1994. Pennsylvania.
- [59] Yilmaz I, Yuksek G. Prediction of the strength and elasticity modulus of gypsum using multiple regression, ANN, and ANFIS models. *Int J Rock Mech Min Sci* 2009;46(4):803–10. <https://doi.org/10.1016/j.ijrmms.2008.09.002>.
- [60] Zorlu K, Gokceoglu C, Ocakoglu F, Nefeslioglu HA, Acikalin S. Prediction of uniaxial compressive strength of sandstones using petrography-based models. *Eng Geol* 2008;96(3):141–58. <https://doi.org/10.1016/j.enggeo.2007.10.009>.
- [61] Nishiura D, Sakai H, Aikawa A, Tsuzuki S, Sakaguchi H. Novel discrete element modeling coupled with finite element method for investigating ballasted railway track dynamics. *Computers and Geotechnics* 2018;96:40–54. <https://doi.org/10.1016/j.compgeo.2017.10.011>.